Journal of Membrane Science 577 (2019) 69–78

Contents lists available at ScienceDirect

Journal of Membrane Science

journal homepage: www.elsevier.com/locate/memsci

Porous poly(vinylidene fluoride) membranes with tailored properties by fast and scalable non-solvent vapor induced phase separation

Clemens Alexowsky[a], Marta Bojarska[a], Mathias Ulbricht[a,b,*]

[a] Lehrstuhl für Technische Chemie II, Universität Duisburg-Essen, Universitätsstr. 5, 45141 Essen, Germany
[b] CENIDE – Center for Nanointegration Duisburg-Essen, NETZ – Nano Energie Technik Zentrum, Carl-Benz Str. 199, 47057 Duisburg, Germany

ARTICLE INFO

Keywords:
Vapor induced phase separation
Poly(vinylidene fluoride)
Dimethyl sulfoxide
Membrane preparation

ABSTRACT

Hydrophobic and highly porous poly(vinylidene fluoride) (PVDF) membranes with isotropic cross section as well as tunable and narrow barrier pore size distribution in the range from ~0.1 to ~1 μm have been prepared using the non-solvent vapor induced phase separation (VIPS) technique. The process conditions have been tuned to suit an industrial scale up, using a short production time and dimethyl sulfoxide (DMSO) as solvent for PVDF, instead of commonly used hazardous chemicals. Factors like kind of solvent, the relative humidity of air, the exposure time to humid air and the mass fraction of PVDF in the casting solutions have been used to tune membrane characteristics. Interestingly, it was revealed that DMSO as a less common solvent for PVDF shows better qualities regarding upscaling than other more frequently used polar aprotic solvents (e.g. dimethylacetamide) when using VIPS under suited conditions. The phenomenon was explained through investigations of the membrane formation step, in particular by water uptake and cloud point measurements, as well as structure and performance analyses, e.g. by scanning electron microscopy, gas flow/liquid dewetting permpometry, gas and water vapor permeability analyses and liquid water entry pressure measurements. Lab-scale manufactured membranes showed pore characteristics and performance desired for membrane contactor applications. Furthermore, fabrication on a roll-to-roll machine using a nonwoven support and the established VIPS conditions was realized in a short manufacturing time; resulting membranes structure and characteristics were found to be similar to the ones for the lab-scale membranes. Overall, the combination of PVDF with DMSO gives promising opportunities for a more eco-friendly industrial fabrication of porous membranes with advanced properties via VIPS.

1. Introduction

Poly(vinylidene fluoride) (PVDF) is widely used to prepare membranes for ultrafiltration and microfiltration [1–3]. Porous and hydrophobic membranes are also utilized for other applications such as membrane distillation or membrane contactors where the membrane has the function to stabilize the interface between an aqueous phase and a gas or other liquid phase [4–10]. For that certain specific properties are required. Barrier pore sizes are mostly between 0.1 and 1 μm, with a narrow pore size distribution; porosity and water contact angle should be high; membrane thickness should be low (at sufficient mechanical stability). These characteristics lead to important performance parameters like liquid (water) entry pressure (LEP) and water vapor transport rate (WVTR). Most commonly such membranes are made from polytetrafluoroethylene (PTFE), PVDF or polypropylene (PP) [11]. In terms of hydrophobicity, PP falls short to PVDF, but the latter is less hydrophobic than PTFE [12]. Still, in many cases, PVDF is the polymer of choice due to its processability in phase separation processes, which makes membrane fabrication easier, scalable and cheaper than for PTFE [1,3,13].

In fact, the production of polymeric membranes is dominated by phase separation methods, most commonly liquid non-solvent induced phase separation (NIPS), due to its versatility for obtaining various pore structures in combination with relatively simple setup and therefore low cost. During NIPS, a cast polymer solution film is directly immersed into a coagulation bath in which membrane formation takes place induced by fast mass transfer and solvent exchange processes in liquid phases. Evolving from that are typically anisotropic porous membranes, with finger pore-like macrovoids and a rather dense top layer [2]. Efforts have been made to achieve bi-continuous lacy structured PVDF membranes by NIPS, for example, via the addition of non-solvents [14–16] or co-solvents [17] to the casting solution, or via mixing water

* Corresponding author at: Lehrstuhl für Technische Chemie II, Universität Duisburg-Essen, Universitätsstr. 5, 45141 Essen, Germany.
E-mail address: mathias.ulbricht@uni-essen.de (M. Ulbricht).

https://doi.org/10.1016/j.memsci.2019.01.033
Received 19 October 2018; Received in revised form 14 January 2019; Accepted 18 January 2019
Available online 26 January 2019
0376-7388/

in the coagulation bath with other (non-)solvents or additives [13,14]. Using the non-solvent vapor induced phase separation (VIPS) method is an alternative [17–19].

VIPS was first patented in 1922 for the preparation of cellulose ester membranes by Zsigmondy and Bachmann [20]. This method involves exposition of the cast polymer solution film to a non-solvent containing atmosphere in order to induced phase separation, after which the polymer film is immersed into a coagulation bath to fix the porous polymer structure and wash out the remaining solvent. Hence, the non-solvent is introduced into the liquid cast film by absorption from the gas phase. The mass transfer through the gas-liquid boundary is slow compared to the mass transfer through the dynamic liquid-liquid boundary during NIPS [21]. A change in the rate of mass transfer influences the morphology of the obtained membrane. Commonly used methods to influence the rate of mass transfer for NIPS are on the one hand manipulating the viscosity of the cast film and on the other hand imposing changes to the coagulation bath such as changing its temperature, choosing the right non-solvent (e.g., water, alcohols) or adding solvent to the coagulation bath [22,23], i.e. manipulating the conditions in the liquid phase. In contrast, besides the temperature of cast film (with direct impact on viscosity), major and unique factors onto mass transfer rate during VIPS are relative humidity, temperature and flow conditions in the vapor phase, and the exposure time of the cast film to the vapor. Indeed, the influence of relative humidity and exposure time during VIPS are reported frequently [24–27], whereas the temperatures during the vapor uptake are rarely in the focus of research [19]. The rate of air flow and the flow geometry in the vapor box are, strangely, not even mentioned in most of the publications about VIPS, although it must be expected that humidity decreases next to the cast polymer solution film and the resulting humidity gradient in the vapor phase is determined by flow conditions.

For PVDF membranes, obtained by VIPS, several distinct kinds of morphologies have been reported, which are a result of variations in parameters like mass fraction of PVDF in the casting solution [28], kind of solvent, PVDF dissolution temperature [18,28], exposure time to water vapor [28] and many others. However, there are significant doubts whether VIPS is suitable for relatively fast roll-to-roll membrane fabrication [6]. In fact, the next challenge after proof of concept in lab scale is to make membrane preparation feasible for industrial production. Important aspects are the option to use a support (e.g. a non-woven), time consumption, safety regulations and the environmental load of the process, all adding to the total production costs of the membrane. Many reported processes for the preparation of hydrophobic and porous PVDF membranes include solvents like dimethylacetamide (DMAc) [29], N-methyl-2-pyrrolidone (NMP) [30] or dimethylformamide (DMF) [31], which are labeled as hazardous substances through the GHS and REACH classifications and will possibly be restricted in industrial use by the EU in the future [32]. Other studies include the use of volatile solvents (e.g. ethanol, acetone) in the coagulation bath [22,33,34] or as a co-solvent [9], which leads to large amounts of waste and difficulties in work safety. Several studies also utilize the VIPS method to produce PVDF membranes but using polar aprotic solvents such as DMAc, NMP, or DMF [17,27–29,35]. In a first, very recent report, Meringolo et al. [36] produced porous and hydrophobic PVDF membranes via VIPS, using DMSO as an alternative solvent and water as a coagulation bath. Although by this means no chemicals of concern were used, thus making the process more industrially applicable, exposure times of the cast film to the non-solvent vapor were larger than 5 min [36]. This would lead to a big footprint in a roll-to-roll setup, as the exposure time in combination with casting speed correlates with the length of the vapor box, necessary in a VIPS setup. In addition, short process times are in general favorable for cost reduction in industry.

In this study, hydrophobic and macroporous PVDF flat-sheet membranes are produced using DMSO as a solvent via VIPS. Although the combination of polymer, solvent and process has already been reported very recently [36], it is now shown, that very short membrane fabrication times, as required by industrial production, are also feasible. Furthermore, deep investigations in tailoring membrane characteristics through variation of process parameters, such as molecular weight of PVDF, dissolution temperature (T_d) for preparing the dope solution or exposure time to non-solvent vapor are done. Finally, the desired membrane structure is also produced on a pilot scale roll-to-roll system using a non-woven as a support. Based on this work, a range of VIPS process conditions will be known for fast and scalable fabrication of porous PVDF membranes with tailored properties.

2. Materials and methods

2.1. Materials

Poly(vinylidene fluoride) (PVDF; Solef 6010, MW 300–320 kDa, and Solef 1015, MW 570–600 kDa, both from Solvay, Rheinberg, Germany) was dried overnight at 80 °C and ~10 mbar in an oven. Dimethylsulfoxide (DMSO; analytical grade, from Carl Roth, Karlsruhe, Germany) and dimethylacetamide (DMAc; analytical grade, from Alfa Aesar, Karlsruhe, Germany) were used as solvents for PVDF as received. Deionized water was used throughout the experiments.

2.2. Preparation of PVDF membranes in lab scale

PVDF was dissolved in the chosen solvent under magnetic stirring for 24 h at a dissolution temperature (T_d) of 50 °C. The solution was then allowed to rest at this temperature for degassing. After cooling down to room temperature (21–23 °C) within about 30 min, the solution did not rest for more than another 30 min until the homogeneous polymer solution was poured on a glass plate. By moving the glass plate at 5 mm/s under a casting knife with a chosen gap, a polymer solution film was generated. This film was immediately afterward exposed to humid air in a “vapor box” (detailed description and image in Fig. S1, Supplementary information). The temperature (21–23 °C) and the air stream (13.7 – 14.4 l/h) inside the box were constant; the humidity and the exposure time were varied. The polymer film was then taken out of the vapor box into a dry atmosphere (relative humidity < 18%) to prevent further uncontrolled water uptake. Finally, the glass plate was put into a coagulation bath, filled with water at constant temperature (20–21 °C) for 24 h. Water was changed once after 30 min of immersion of the film. Cut membrane samples were dried in a freeze drier at 0.110 mbar and − 18 °C for 24 h.

In case of casting at temperatures above room temperature, the degassed solution was cooled down to the chosen casting temperature (T_{cast}) or directly used for membrane preparation if T_d and T_{cast} were equal. Casting was then done on a pre-heated glass plate on a casting machine (Coatmaster 509 MC, Erichsen, Hemer, Germany) (in contrast to casting at room temperature) and a relative humidity of less than 18%. After that, the cast film on the glass plate was put into set humid air atmosphere as described above.

2.3. Preparation of PVDF membranes on a pilot scale roll-to-roll system

PVDF was dissolved in DMSO with the help of an overhead stirrer at constant stirring rate for 2 h at 50 °C. After degassing under vacuum, the solution was cooled down to room temperature. Membranes were produced on a Click-and-Coat® roll-to-roll system (Coatema, Dormagen, Germany) on a PET support (kindly supplied by GVS S.p.A., Zola Predosa, Italy). The used exchangeable modules of the casting system were: 1. unwinder, 2. stretching, 3. coating, 4. vapor box, 5. coagulation bath, 6. IR dryer, 7. rewinder. The vapor box measured 2 × 1 × 0.8 m and was supplied with humid air by a PH professional humidifier (Franco HVAC Technologies, Cervasca, Italy). The polymer solution was poured next to the casting knife with a gap height of 150 µm. Further casting parameters like support tension, running speed

(and as a result exposure time to humidity), casting height, relative humidity and drying temperature were set individually for each run. For further information about the setup see Fig. S2 and Fig. S3 in Supplementary information.

2.4. Characterization of casting solutions

Dynamic viscosity of the casting solutions was measured on an Anton Paar Physica MCR301 rheometer using the CP-25 geometry and varying shear rate from 0.1 to 1000 s^{-1} at 25 °C.

Cloud point measurements were done to achieve data for a binodal curve in a ternary phase diagram. 40 g of polymer solution were heated up to 120 °C under reflux. After cooling down to 80 °C, water was added in 100 µl steps. Once the agglomerates had dissolved the solution was cooled down to 25 °C and the turbidity of the solution was observed by eye. Addition of water at 80 °C and observing the turbidity at 25 °C were repeated until the solution showed a cloudy appearance.

Water uptake of the cast polymer film was measured gravimetrically. Casting was done as described above (cf. Section 2.2). Immediately thereafter, the glass plate with the polymer film was weighed, then exposed to the humid air in the vapor box for a certain time (cf. Section 2.2) and weighed again. The resulting data is the mass of water taken up per square meter of a cast polymer solution film (of known thickness).

2.5. Characterization of membranes

Membrane thickness was measured with a micrometer screw at least at three positions of the membrane and verified by scanning electron microscopy cross-section analysis.

Scanning electron microscopy (SEM) images were obtained with help of an ESEM Quanta 400 FEG instrument operating at high vacuum. Membrane samples were coated with platinum using a sputter coater (K-550, Emitech Ltd., Kent, UK) at 20 mA for 1 min. For cross-section images, samples were broken after cooling with liquid nitrogen.

Volume porosity was estimated gravimetrically by filling the pores of the membrane with a fluorinated liquid (Galwick®) and calculating porosity, ε (%), according to Eq. (1):

$$\varepsilon = \frac{m_{wet} - m_{dry}}{\rho A \delta} \times 100\% \quad (1)$$

Where ρ (g/cm^3) is the density of Galwick®, A (cm^2) and δ (cm) are the area and thickness of the membrane sample, m_{wet} (g) and m_{dry} (g) are the wet and dry sample weights.

Pore size and *pore size distribution* as well as the *air flow* through the membrane were measured by a capillary flow porometer (CFP, Porous Materials Inc., Ithaca, USA) as part of or via the gas flow/liquid displacement method. As wetting liquid Galwick® (surface tension 15.9 dynes/cm) was used. All samples were analyzed by the "wet up"/"dry up" method, assuming a shape (tortuosity) factor of 1.

Liquid entry pressure (LEP) of membranes was measured on a simple device made in the universities workshop. The membrane sample with the active side down was fixed on a container filled with water. Pressure on the water reservoir was applied through compressed air. The pressure was increased in 0.1 bar steps and allowed to remain constant for 10 s. Once a water droplet was detected visually on the support side of the membrane, the liquid entry pressure was reached.

Water vapor transport rate (WVTR) is one possible measure to quantify the flow of water vapor through a fabric [37]. The set-up is shown in Fig. S4 in Supplementary information. The membrane sample was fixed between two PTFE sample holders and sealed by several O-rings. The upper active side was exposed to an aqueous lithium chloride solution (400 g/L), providing the driving force for water vapor transport through the membrane. To minimize influence of dilution by absorbed water, the liquid volume in the reservoir (32 mL) in contact with the membrane was continuously exchanged with a large supply of lithium chloride solution (140 mL) through a peristaltic pump with the flow rate of about 3.9 mL/min. On the lower side of the membrane a precisely weighed amount of deionized water was heated to 50 °C in a glass cylinder (100 mL) filled on the bottom with liquid. From the surface of the liquid to the membrane, the water vapor cooled down to room temperature by that generating a water vapor saturated atmosphere next to the membrane. Unsupported membrane samples were put on a piece of PET non-woven to enhance mechanical stability and to allow direct comparison between samples prepared with or without non-woven support. After at least 20 h, the remaining liquid water in the glass cylinder was weighed again. The weight difference, the membrane area and elapsed time yield the WVTR (g/m^{2}h).

3. Results and discussion

3.1. Solvent effect on PVDF membrane structure

For membrane preparation the choice of solvent is fundamental and crucial for the design of the whole process. Commonly used solvents in membrane preparation via phase separation of polymer solutions are DMAc and NMP, but those are now described as substances of very high concern (SVHC) by GHS or REACH [32]. Hence, there is a need to substitute these solvents with less hazardous chemicals and at the same time retain or even improve desired characteristics of the resulting membrane. The quality of the polymer solvent can be judged by the differences of the Hansen solubility parameters for PVDF and the respective solvent. Interactions via dispersive, polar and hydrogen bonding forces are considered for polymer and solvent. With the help of Eq. (2), the difference can be calculated [38]. The smaller the difference, the better is the solvent quality. As it is shown in Table 1, DMSO shows clearly worse ability to dissolve PVDF compared to three other commonly used polar aprotic solvents. This is probably the reason, why DMSO is less often used for the fabrication of PVDF membranes than DMAc or NMP, which can dissolve the commonly used fractions of PVDF (< 20%) at room temperature (what is not the case for DMSO; see below).

$$\Delta\delta_{p-s} = [(\delta_{dp}-\delta_{ds})^2 + (\delta_{pp}-\delta_{ps})^2 + (\delta_{hp}-\delta_{hs})^2]^{1/2} \quad (2)$$

$\Delta\delta_{p\text{-}s}$ – difference of Hansen solubility parameters (HSP) for polymer and solvent, δ_d – contribution of dispersion forces to HSP, δ_p – contribution of polar forces to HSP, δ_h – contribution of hydrogen bonds to HSP; the second indices "p" and "s" stand for polymer and solvent, respectively.

Specifically, for PVDF, the temperature at which the polymer is dissolved plays also a crucial role for the resulting membrane morphology. As a semi-crystalline polymer, PVDF can appear in different crystalline phases; most relevant are alpha and beta forms. Crystallization has also an influence on the formation of the pore structure because it can compete with liquid-liquid demixing; to what extent this happens and which of the two phases is predominately obtained after phase separation is also determined by the dissolution temperature (T_d). Li et al. [18] identified a critical dissolution temperature (T_{cd}), where under VIPS conditions a marked change of membrane pore morphology occurred. For membranes prepared from solutions made below T_{cd}, PVDF crystallized in both, alpha and beta

Table 1
Hansen solubility parameters of PVDF, DMAc, NMP, DMF and DMSO as well as differences in HSP between PVDF and these commonly used solvents [38].

	δ_d	δ_p	δ_h	$\delta_{p\text{-}s}$
PVDF	17.2	12.5	9.2	–
DMAc	16.8	11.5	10.2	**1.47**
NMP	18.0	12.3	7.2	**2.16**
DMF	17.4	13.7	11.3	**2.43**
DMSO	18.4	16.4	10.2	**4.20**

forms and bicontinuous, lacy pore structures with high mechanical stability were obtained. For analogous polymer solutions prepared above T_{cd} under same VIPS conditions, the alpha phase vanished with increasing T_d and the membrane morphology changed to a nodular structure with poor interconnectivity and mechanical strength. It has also been found for the solvents DMAc, NMP and DMF that in the range of PVDF concentrations suited for preparation of porous membranes by VIPS, T_{cd} was always somewhat higher than the minimum dissolution temperature (T_{min}), i.e. the temperature required to obtain a homogeneous polymer solution [18]. Both temperatures increased with decreasing solvent quality; for DMF as the least good solvent for PVDF in the work by Li et al. [18] (cf. Table 1), T_{cr} was found to be between 30 and 40 °C for PVDF fractions of 14–18%. It should be noted that the importance of the dissolution temperature for PVDF had already earlier been demonstrated and discussed in the context of membrane formation via NIPS [39]. In this study, with DMSO as solvent, T_d (50 °C) was always below T_{cd}. Except where stated, the film casting was done at room temperature where all polymer solutions in DMSO used in this study are metastable ($T < T_{min}$). Resulting membranes were semi-crystalline and both alpha and beta forms could be identified, for instance with IR spectroscopy; larger exposure time to water vapor lead to an increase of the alpha to beta ratio (Fig. S5, Supplementary information). Results for membrane preparation with PVDF solutions in DMSO prepared at $T_d > T_{cd}$ leading to nodular morphologies, and the influence of the dissolution time and other VIPS parameters with such systems will be subject of another publication.

First, the influences of the polymer solvent in combination with VIPS exposure time are presented. Cast films from solutions of 15% PVDF Solef 6010 in DMAc or DMSO were exposed to 80% relative humidity for different exposure times (t_{VIPS}) of 1, 2 and 6 min. As can be seen in the SEM micrographs in Fig. 1, the use of DMAc results in the commonly known finger-like macrovoids and a dense top layer for t_{VIPS} = 1 min. This indicates clearly that phase separation proceeds presumably via NIPS, i.e. the structure is formed only upon contact with the liquid non-solvent coagulation bath. By increasing t_{VIPS} to 2 min, the cross-section shows a sponge-like structure, but the top layer remains dense. Only after 6 min, the desired structure (sponge-like and open porous) is achieved. If DMSO is used as solvent, the favored isotropic sponge-like structure is achieved already after t_{VIPS} = 1 min.

These results can be related to the different solvent qualities for PVDF. A film cast from a solution of PVDF in DMSO is more likely to undergo phase separation than an analogous film cast from a solution PVDF in DMAc. In turn, this provides very interesting opportunities for VIPS because membrane fabrication times could be relatively short (similar to NIPS which takes not more than 1 min between casting and phase separation; cf. Fig. 1 above).

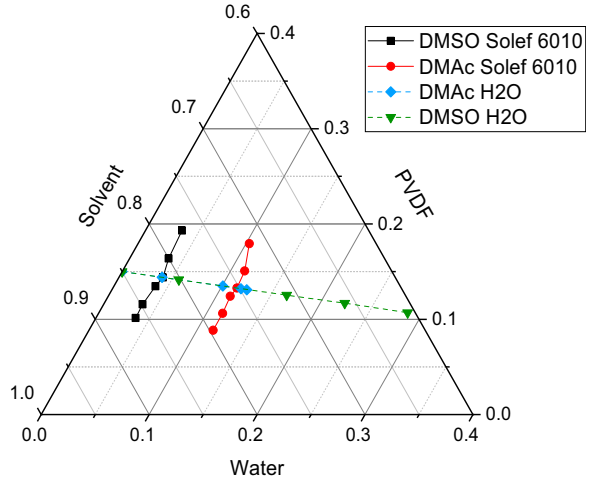

Fig. 2. Ternary phase diagram showing binodal lines for PVDF/DMSO/water (black squares) and PVDF/DMAc/water (red circles) as well as the water uptake from 80% RH of 200 µm cast films of PVDF in DMSO (green triangles) and PVDF in DMAc (blue diamonds), for 0, 2, 6, 11, and 21 min.

Furthermore, the pathway and rate of membrane formation process are not only determined by the quality of the polymer solution. The affinity of the solvent to the non-solvent (water) also plays a significant role. To estimate the ability how well solvent and non-solvent mix, calculations of free mixing enthalpies were performed by Wei [40]. According to the results, DMSO mixes much better with water than the other three solvents DMAc, NMP and DMF.

In order to obtain information about the mutual interactions between polymer, solvent and non-solvent, cloud point measurements of PVDF solutions in DMSO and DMAc were performed. Initial concentrations of PVDF Solef 6010 (similar results were found for Solef 1015) in solution were 10%, 12%, 14%, 15%, 17% and 20%. The obtained data are depicted in a fraction of a ternary phase diagram in

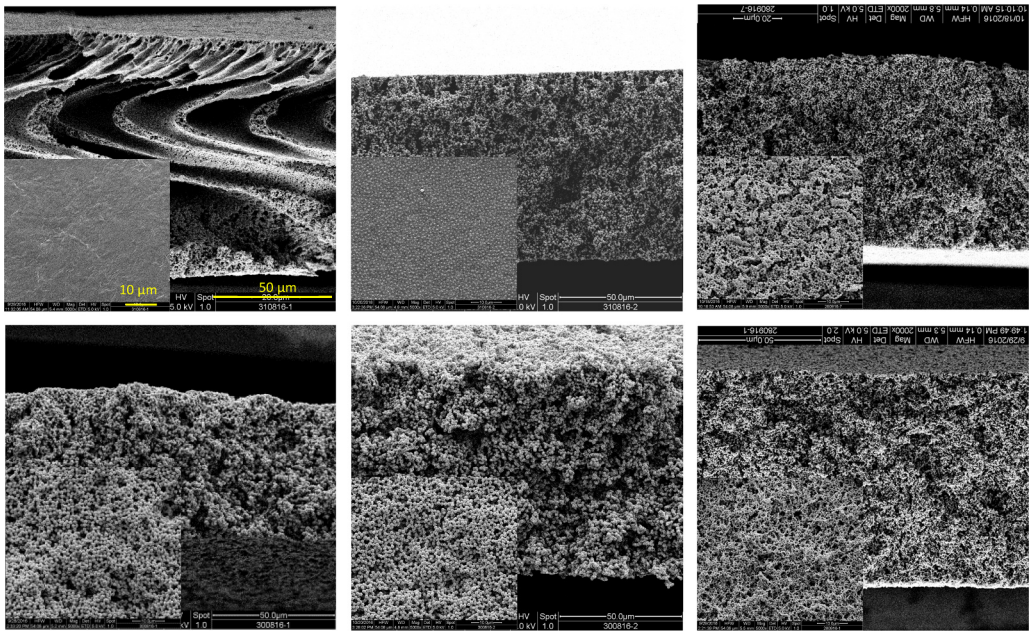

Fig. 1. SEM images of PVDF membranes (cross-section 2k magnification, top view inserted 5k magnification, scale bars valid for all images) obtained after using DMAc (top row) and DMSO (bottom row) as solvent in a solution of 15% PVDF Solef 6010 at 80% relative humidity. From left to right exposure time to water vapor, t_{VIPS}, 1 min, 2 min and 6 min.

Table 2
Comparison of the ability of non-solvent (NS) water to destabilize the solution of PVDF (P) in the respective solvent (S), i.e. binodal composition with 15% PVDF Solef 6010 (from Fig. 2), average affinity between S and NS (calculated from data in [40]), dynamic viscosity of 15% PVDF solutions at 5 s^{-1}, fraction of water after 20 min exposure of cast PVDF solutions films to 80% RH as well as interpolated exposure time needed to reach the binodal composition (from Fig. 2), all for either DMAc or DMSO as solvent.

Solvent	Fraction of NS to destab. P-S [%]	Affinity NS-S; rel. ΔG_{mix} [-]	Viscosity of P-S [Pa·s]	Fraction of NS after 20 min [%]	Time to destab. P-S; t_{VIPS} [min]
DMAc	11.5	0.5	0.61	12	6–11
DMSO	4.1	− 0.1	1.99	29	< 1

Fig. 2. The binodal curve of DMSO solutions is located left of that for DMAc solutions, which is in agreement with the differences of Hansen solubility parameters (cf. Table 1). In addition, water uptake by the 200 µm thick cast films of 15% PVDF Solef 6010 solutions at a relative humidity (RH) of 80% and t_{VIPS} of 2, 6, 11 and 21 min was measured and is also shown in Fig. 2. It is very clearly seen that in the same time of exposure to humid air, a cast film made with DMSO takes up much more water than a cast film made with DMAc. This can be explained by the higher affinity between DMSO and water (cf. above). Consequently, cast films of PVDF in DMSO undergo phase separation much faster than those in DMAc because of the less good solvent quality of DMSO for PVDF and its higher affinity for water.

The formation of porous membrane structures can be determined by thermodynamic factors such as affinities between polymer and solvent as well as between of solvent and non-solvent, but also by kinetic factors with the viscosity of the polymer solution as main contribution. Measured viscosity data for 15% PVDF Solef 6010 solutions made from DMAc and DMSO is shown in Table 2 together with the cloud point, i.e. water fraction at binodal composition, for these solutions as well as a calculated average for non-solvent solvent affinity from the publication of Wei [40]. In addition, the experimentally determined fractions of water after t_{VIPS} = 20 min and the estimated values for t_{VIPS} needed to reach the binodal composition are also shown. Much higher water uptake and much earlier crossing of the binodal line for solutions prepared from DMSO compared to those from DMAc show, that affinity is the dominating effect over viscosity (which is higher for solutions in DMSO compared to those in DMAc). Furthermore, it will be shown and discussed later (Section 3.4) that a change of solution viscosity by different concentrations of PVDF in DMSO did not have an influence onto the rate of water uptake within the first 10 min of exposure to water vapor. Hence, structure formation of the membranes for relatively short exposure times which are sufficient to induce phase separation (cf. Fig. 2) is determined by thermodynamics. Overall, membranes made with PVDF/DMSO require significantly shorter t_{VIPS} in order to achieve the desired porous structure compared to membranes made with PVDF/DMAc.

3.2. Effects of relative humidity of the vapor phase on membrane structure

Besides solvent and its effect onto the required exposure time to induce VIPS, the relative humidity of the atmosphere during the VIPS process plays a central role. This parameter determines the driving force for water absorption and how much water is available to be absorbed by the cast film. The design and construction of the vapor box (cf. Section 2.2) had been done so that the volume of the gas phase in relation to the area of the cast film along with the renewal of the atmosphere by efficient vapor supply from the humidifier lead to almost constant water vapor pressure (relative humidity) in the gas phase, so that the effect on driving force should be dominating. PVDF Solef 6010/DMSO solutions with 15% polymer fraction were exposed for 1 min to air with 20%, 40%, 60% and 80% relative humidity. SEM images in Fig. 3 show that low humidity (20%) results in anisotropic membranes with dense top layer and finger-like macrovoids (similar to what had been obtained from PVDF Solef 6010/DMAc after the same time at 80% RH; cf. Fig. 1). At 40% RH the cross-section is sponge-like, but the top layer is still not highly porous. At 60% and 80% RH, the desired isotropic sponge-like cross-section morphology with an open porous surface is achieved.

For a better understanding of the VIPS process, the water uptake of polymer films cast at same thickness from a 15% PVDF Solef 6010/DMSO solution at 1 min exposure was measured at 20%, 40%, 60% and 80% relative humidity. The water uptake increased from 2 over 9 and

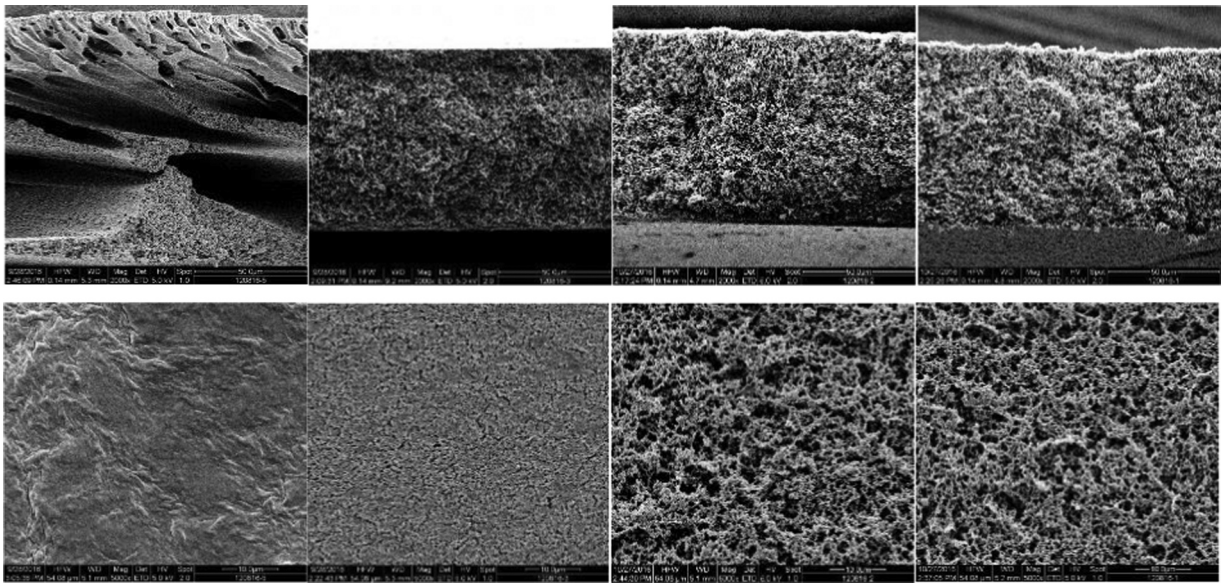

Fig. 3. SEM images of PVDF Solef 6010 membranes prepared from solutions with 15% polymer fraction (top row - cross-section 2k magnification; bottom row - top view 5k magnification) cast at 20%, 40%, 60% and 80% (left to right) relative humidity and an exposure time of 1 min.

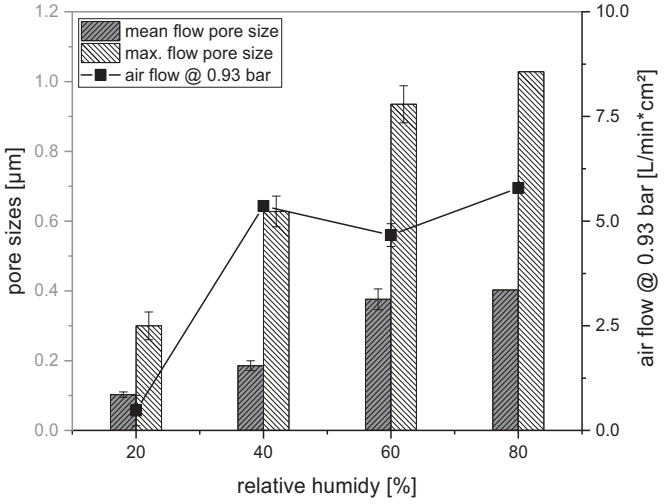

Fig. 4. Gas flow/liquid dewetting permporometry data for PVDF Solef 6010 membranes prepared from solution with 15% polymer fraction in DMSO and exposure time of 1 min at 20%, 40%, 60% and 80% relative humidity.

19 to 34 g/m^2, respectively. The expected proportional relation was found, the higher the humidity in the vapor phase, the higher the difference of the chemical potential for water between gas and liquid phase (polymer solution film). Furthermore, the water uptake can be expressed in mass fraction in the ternary system with PVDF and DMSO (see Fig. S6 in Supplementary information). The cast film after 5 min of exposure at 40% relative humidity contained about 4% water which matches roughly the binodal composition in Fig. 2. Apparently, a higher humidity in combination with the same exposure time will be sufficient to induce phase separation already before immersion in the coagulation bath, thus enabling formation of the isotropic cross-section morphology (cf. Fig. 3).

More information about membrane characteristics was gained through permporometry measurements. Fig. 4 shows maximum and mean flow pore sizes, as well as the air flow through the membranes prepared from a 15% PVDF Solef 6010/DMSO casting solution with t_{VIPS} = 1 min at RH of 20%, 40%, 60% and 80%.

Pore sizes and air flow increase with increasing relative humidity. The much lower air flow measured for the lowest humidity compared to the other membranes and the more systematic trend for pore sizes may be explained by the fact that a rather dense top layer had been formed for this particular membrane (cf. Fig. 3).

The absorption of water in the polymer film is faster for higher humidity, due to a higher difference in chemical potential (cf. above). Under such conditions, pores are formed through nucleation and growth of the polymer lean phase. As more water is present for higher humidity, the polymer lean phase grows faster compared to the scenario at lower humidity. This results in bigger pores, as had also been found by AlMarzooqi et al. [29].

In case of NIPS, Strathmann and Kock argued, that exchange of non-solvent and solvent at the top of the cast film is fast compared to diffusion of non-solvent from the surface into the bulk of the cast film [41]. Hence, a dense top layer is formed through rapid phase separation at the surface of the cast film, hindering diffusion of non-solvent into the bulk leading to an anisotropic cross-section. In case of VIPS, the uptake of water from the gas phase is much slower. As water is absorbed in the surface layer of the cast film, a concentration profile evolves. However, still, the concentration of water at the top of the cast film is not high enough to initiate phase separation. Therefore, diffusion of water into the bulk of the cast film proceeds so that water concentration in the film is rising evenly, ultimately leading to a (mostly) isotropic pore structure. Membranes cast at 20% relative humidity show no structural characteristics typical for VIPS. The water uptake from the vapor phase in short time is not high enough to initiate pore forming before immersion in the coagulation bath. At 40% relative humidity, the water uptake from the atmosphere is already high enough, so that a significant amount of water can diffuse into the bulk of the cast film. Still, however, phase separation did not solidify the final structure so that only after the immersion into the coagulation bath a dense top layer is formed. Higher humidity (60% and 80%) lead to an open porous surface with sponge like cross-section. Water uptake during the VIPS step is so high, that the formed structure solidifies already and the consecutive immersion into a water bath does not lead to phase separation at the top of the polymer film.

3.3. Effects of film casting above room temperature

In Fig. 5, SEM images show the membrane structure obtained as consequence of varied casting temperature, from room temperature to 40 and 50 °C, at two different times of exposure to humid air.

An open porous surface with a sponge-like cross-section morphology can be observed after casting at room temperature as well as at 40 °C at the given exposure times to humid air. If the casting temperature is elevated to 50 °C, t_{VIPS} = 2 min results in a dense top layer and finger-like macro-voids, in contrast to t_{VIPS} = 6 min which again results in the desired open porous sponge-like morphology. Having in mind the effects of temperature and solution quality, it seems obvious, that PVDF solutions cast at higher temperature are increasingly more stable. Hence, more water will be needed to reach the unstable region where porous morphology is formed by phase separation. However, in addition, the water uptake at elevated casting temperature was found to be much lower than at room temperature. A 200 µm thick film cast of a 15% PVDF Solef 6010/DMSO solution within an exposure time of 5 min takes up about 34 g/m^2 of water when the casting is done at room temperature. Under otherwise same conditions (including temperature and relative humidity in the gas phase), but with 50 °C casting temperature, only about 10 g/m^2 water is absorbed in the polymer solution film. This is the consequence of the lowered chemical potential difference between gas phase and cast film and the increase of water vapor pressure with temperature (when temperature of the film is higher than temperature in the bulk of the gas phase, temperature in the gas side boundary layer will be somewhat higher). This had not been studied in more detail, but it is obvious that a lower casting temperature favors the formation of the desired open porous sponge-like membrane morphology. Higher casting temperatures, where PVDF/DMSO solutions are increasingly stable, could be favored in industrial processes because the polymer solution could be stored for longer time before casting. For that, the VIPS conditions must (and can) be adapted.

3.4. Effects of polymer solution concentration and exposure time to water vapor

Fig. 6 shows the maximum pore sizes of membranes made of 14% and 15% PVDF Solef 6010 in DMSO solutions. The biggest pores of 14% PVDF membranes are about 0.2 µm larger than those of membranes prepared from 15% PVDF for all exposure times to humid air. Analogous trends have been found for the mean flow pore diameter (not shown). A lower polymer concentration results in lower viscosity and therefore the mobility of polymer chains is enhanced. Table 3 shows viscosity data for 14% (1.4 Pa s) and 15% (2.0 Pa s) low molecular weight PVDF solutions made with DMSO. Hence, it could seem obvious that this, via higher growth rate of polymer lean phase domains, is the reason for the increase of pore size. Similar results have been found in literature [29]. However, as it is shown later in Section 3.5, a change of viscosity through variation of molecular weight of the polymer does not result in the same trend with respect to changes of pore size. In order to gain further insight, water uptake for cast films containing 12, 13, 14% and 15% PVDF in DMSO was measured (Fig. 7). As expected, water uptake increased with exposure time. However, at 2, 6, and 11 min of

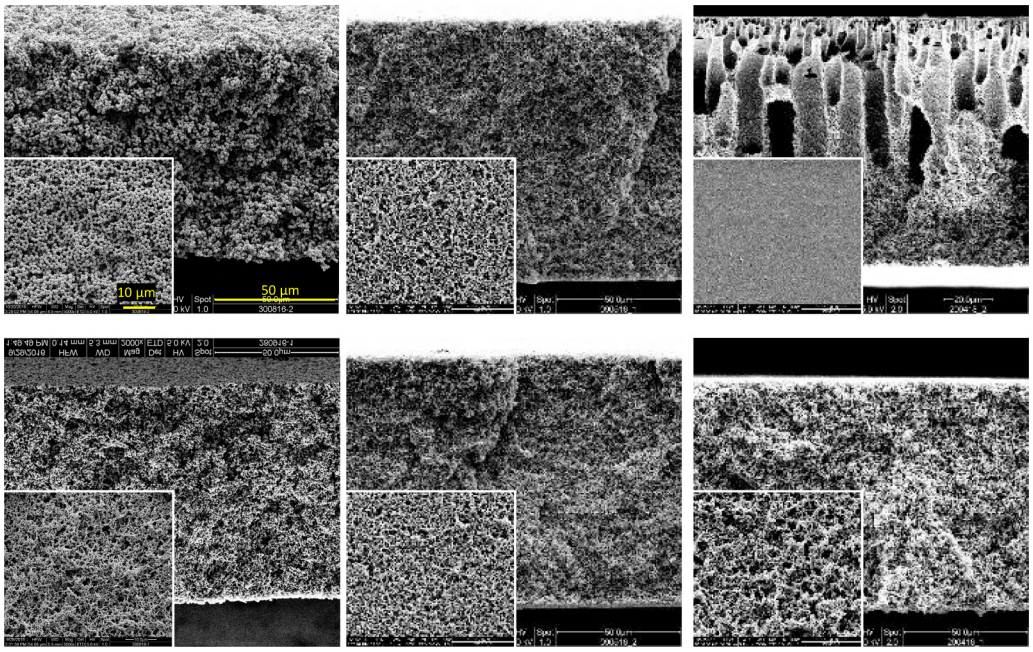

Fig. 5. Cross-section (2k magnification) SEM images of membranes prepared from 15% PVDF Solef 6010 solutions, cast at varying temperature (left – room temperature; middle – 40 °C; right – 50 °C) with 2 min (top row) and 6 min (bottom row) exposure to humid air at 80% RH (top view – 2k magnification – SEM data inserted at lower left of each image).

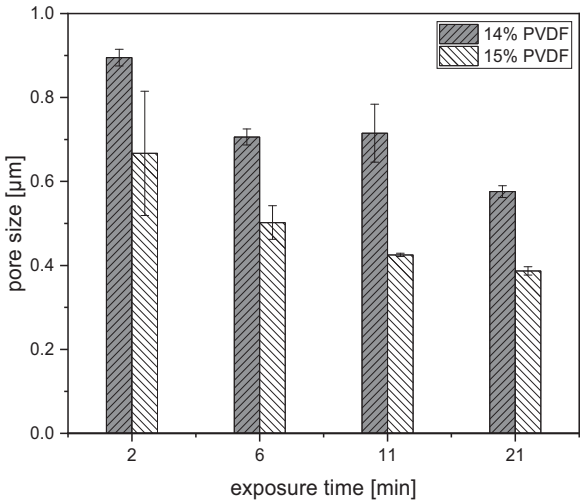

Fig. 6. Maximum pore sizes of membranes obtained from polymer solutions containing 14% and 15% PVDF Solef 6010 in DMSO at different exposure times to water vapor at 80% relative humidity, measured by gas flow/liquid dewetting permporometry.

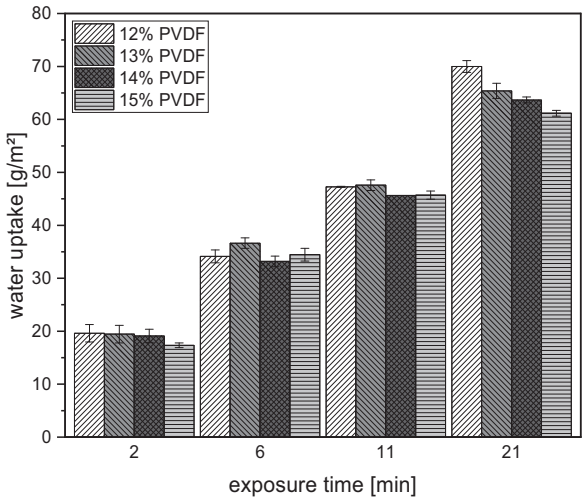

Fig. 7. Water uptake by 200 µm thick cast films of solutions containing different mass fraction PVDF Solef 6010 in DMSO at different exposure times to water vapor at 80% relative humidity.

Table 3
Dynamic viscosity of solutions in DMSO of PVDF of molecular weight and at different concentration.

Polymer	PVDF mass fraction (%)	Viscosity [Pa s]
PVDF Solef 6010	14	1.4
PVDF Solef 6010	15	2.0
PVDF Solef 1015	15	38

exposure to humid air, no significant effect of mass fraction of PVDF in the film on water uptake was found. Only for 21 min of exposure to humid air, water uptake was decreasing with increasing mass fraction of PVDF in the film. Interpretations will be given in conjunction with those for results found for variations in PVDF molecular weight in Section 3.5.

In contrast to results for membrane formation via VIPS by, for instance, Zhao et al. [28] and Zhu et al. [42], the pore sizes decrease with increasing exposure time to humid air. However, Zhu et al. [43] also published results for membrane formation via VIPS where pore sizes decreased with increasing exposure time to humid air. However, in this case the polymer system and the resulting formation processes were more complex compared to the simple ternary system of the present work. Meringolo et al. [36] found increasing pore size of PVDF membranes for up to 5 min exposure time to humid air and smaller pores for 10 and 20 min. The interpretation was that condensation of water on the surface of the cast film at longer exposure time lead to a local NIPS process. Furthermore, Tsai et al. [25] investigated poly(methyl methacrylate) membranes made via VIPS and showed that pore morphology changes from a lacy-like structure to a cellular structure, and therefore barrier pore sizes change also in a non-proportional way as function of VIPS time.

Small water drops on the surface of the cast film were observed by eye in most cases, even at exposure times of 1 or 2 min. However, even after such conditions volume porosity of the membranes was very high (> 90%) and no dense regions as assumed by Meringolo et al. [36]

were found in SEM micrographs. The very good miscibility of water and DMSO [40] supports the idea, that mixing of water and DMSO is relatively fast, and therefore conditions for a local NIPS process are not given. Tsai et al. described coarsening of phase-separated polymer domains in other polymer systems [25]; i.e. a nascent lacy structure showed collapse and coarsening of the polymer rich phase at the surface of the membrane. According to Aarts et al. [44], the growth rate of a domain can be described with help of the solutions viscosity and the interfacial tension. Implying that pores grow in a nucleation and growth mechanism of the polymer lean phase only in the first seconds, coarsening due to above described factors can happen after the first minute of VIPS under the conditions in the present work. Coherent with that, viscosity changes (e.g., due to different concentration of PVDF; cf. Table 3) directly affect the pore sizes in the observed way (cf. Fig. 6).

3.5. Effect of PVDF molecular weight

In addition to the PVDF with low molecular weight (Solef 6010; 300–320 kDa) used in the experiments described in the previous sections, PVDF with very high molecular weight (Solef 1015; 570–600 kDa) was also used. Fig. 8 shows that mean flow and maximum pore sizes increase by about 0.2 µm with Solef 1015 compared to Solef 6010 for long exposure time to water vapor; additional SEM images are provided in Fig. S7 in Supplementary information. Consequently, the air flow is also much larger for the membranes from Solef 1015. It may be expected that higher viscosity of polymer solution leads to a lower mobility of polymer chains as well as lower diffusion of non-solvent into the bulk of the polymer film and thus slower pore forming in a nucleation and growth mechanism of the polymer lean phase. However, considering the interpretation of the influence of exposure time in Section 3.4 and the findings of Aarts et al. [44], coarsening can play a role as well. As described in Ref. [44], viscosity plays a central role regarding the phenomenon of coarsening. A higher viscosity would then prevent a nascent lacy structure from coarsening and therefore result in larger pores. Solutions made from 15% polymer in DMSO had a dynamic viscosity of 2 Pa s for Solef 6010 and 38 Pa s for Solef 1015 (Table 3). Overall, it seems plausible, that bigger pores are formed for smaller polymer concentration, because polymer chains have more space to move. The absolute difference in viscosity between 14% and 15% PVDF Solef 6010 solutions is not very high compared to the difference when increasing the molecular weight (cf. Table 3). For solutions with high viscosity the diffusion rate of non-solvent into the bulk of the polymer is low; therefore resulting in smaller pore sizes for short exposure time. For longer exposure times and low diffusion rate of non-solvent, the polymer lean phase has time to coarse forming larger pores (cf. Fig. 8).

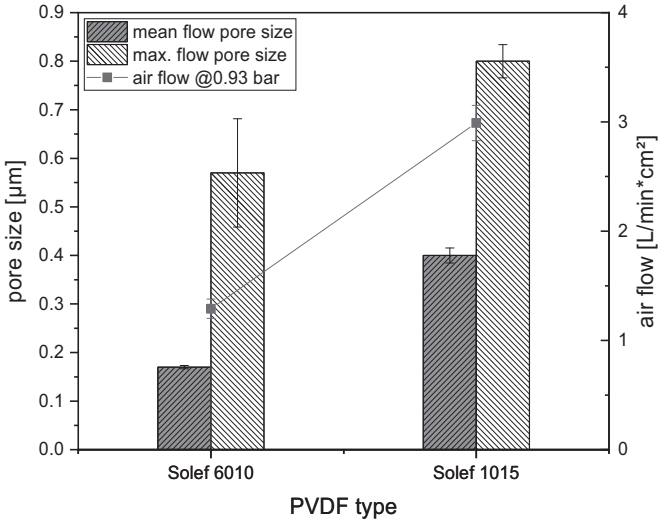

Fig. 8. Mean flow and maximum pore sizes of membranes as well as air flow through membranes made from solutions of 15% PVDF of different molecular weight in DMSO.

Table 4
Characteristics of a newly developed porous PVDF membrane prepared in lab scale.

	Mean	Deviation ±
Porosity [%]	89.2	2.0
Thickness [µm]	98.4	2.8
Mean flow pore size [µm]	0.24	0.01
Maximum flow pore size [µm]	0.59	0.03
Air flow @ 0.93 bar [L/min cm^2]	2.2	0.18
LEP [bar]	2.7	0.16
WVTR [g/m^{2}h]	250	6

3.6. Porous PVDF membranes prepared by VIPS in lab scale

Sections 3.1–3.5 show that tuning of membrane characteristics is possible through several parameters in the VIPS process. For a potential application in a special gas/liquid contactor, a membrane with mean flow pore size of 0.2 µm, narrow pore size distribution, a thickness of less than 200 µm, and having liquid (water) entry pressure (LEP) > 1 bar and a high water vapor transport rate (WVTR) had been targeted. A newly developed prototype membrane obtained with tuned VIPS parameters shows the desired characteristics (Table 4). This prototype membrane can be obtained with good reproducibility which is shown with pore size distributions for different batches in Fig. 9. This membrane was prepared with a solution containing 15% PVDF of low molecular weight (Solef 6010) in DMSO, dissolved at 50 °C for 24 h. The polymer film was cast at room temperature at a thickness of 200 µm and exposed to water vapor at 80% relative humidity for 1 min.

3.7. Supported porous PVDF membranes prepared by VIPS in pilot scale

For further improvement of membrane properties, the fabrication of the self-supporting membrane from lab-scale (cf. Section 3.6) was transferred to a roll-to-roll casting system. Film casting thickness can be reduced because mechanical support is supplied by a non-woven and as a result separation performance (in particular the relation between LEP and WVTR) could be increased.

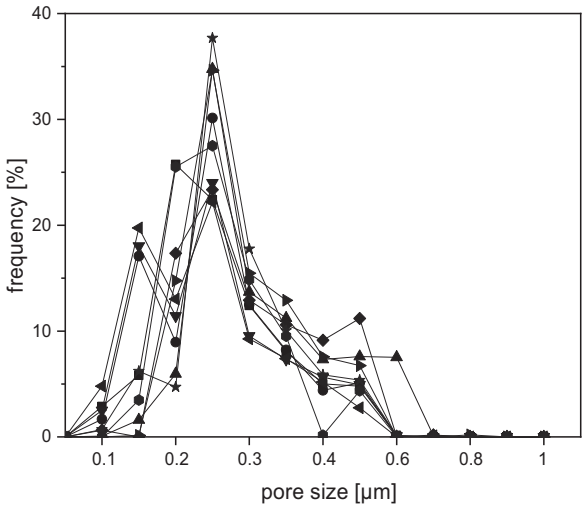

Fig. 9. Pore size distributions (percentage of pores in respective size range) from gas flow/liquid dewetting permporometry of nine separately prepared lab scale batches of the newly developed porous PVDF membrane.

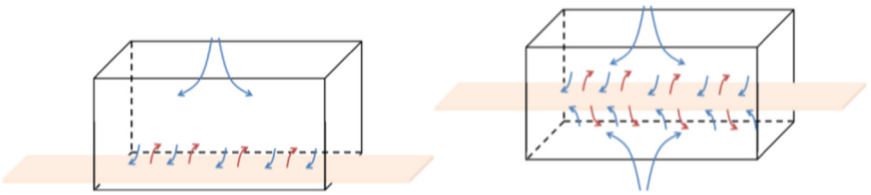

Fig. 10. Schematic design of vapor box; in lab scale with cast film on glass support (left), in pilot scale roll-to-roll system with cast film supported by macro-porous nonwoven (right).

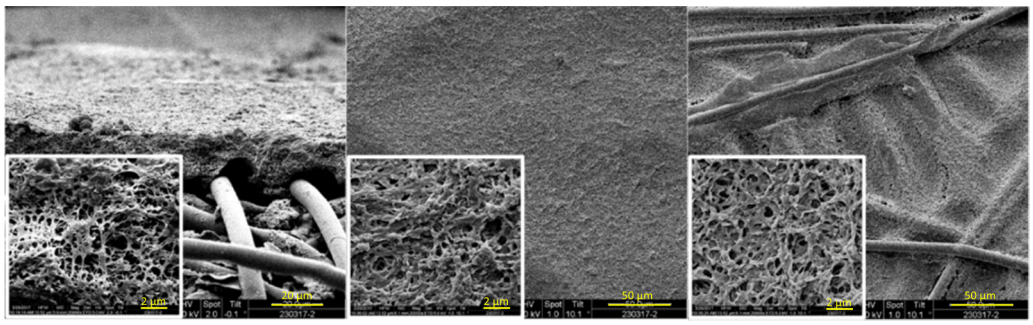

Fig. 11. SEM images of PVDF Solef 6010 membranes fabricated via VIPS on a roll-to-roll system on a PET nonwoven support. Cross-section (left, 2k magnification), top-view (middle, 1k magnification) and bottom-view (right, 1k magnification); higher magnification (20k) images inserted.

All investigations had confirmed that the uptake of water from the vapor phase in the liquid film of the polymer solution is of crucial importance. Hence, the water uptake as function of casting thickness was measured. It was found, that within a fixed VIPS time of 2 min at RH = 80% (room temperature), the water uptake by the cast film does not further increase when the film thickness is larger than 300 µm (see Fig. S7 in Supplementary information). The relative humidity in the gas phase did not change (cf. Sections 2.2 and 3.2); this indicates clearly that water uptake is limited by the mass transfer through the surface of the cast film, with the main resistance on the liquid side. As discussed in Sections 3.1–3.4, fast mass transfer for water is essential for the formation of a membrane with isotropic pore structure within short fabrication time. Therefore, the setup for the preparation of supported membranes was improved by a different design of the "vapor box" for the pilot scale set up, which was possible due to the fact that the cast film is supported by a non-woven instead of a glass plate. The cast polymer film was exposed to humid air from two sides instead of just from the top as in the lab scale preparations (Fig. 10). By that, exposure time to humid air can be minimized.

Fig. 11 shows SEM images of membranes made on the roll-to-roll system. Cross-section and top view display clearly that a bi-continuous lacy structure is obtained. The bottom view shows, that the polymer solution wetted the whole nonwoven support. Overall, an isotropic porous PVDF membrane with an integrated mechanical support had been obtained.

Table 5 shows the characteristics of the supported porous PVDF membranes. Ranges are reported indicating that there were still variations which can be related to fluctuations in process conditions and variability of structure and property over the large fabricated membrane area. Mean flow and maximum pore sizes are somewhat smaller than after lab-scale fabrication. However, the pore size distribution is more narrow, and the LEP can be largely enhanced.

For a possible application in a gas/liquid contactor, LEP and WVTR are two important parameters which give a good impression about the membranes performance with respect to the commonly observed trade-off between barrier and transport properties [37]. That better barrier properties (higher LEP) could be achieved at same permeability (WVTR) indicates that the good performance of the membrane developed in lab scale had been further improved by fabrication in pilot scale. A comparison of the two prototype membranes from lab and pilot scale with commercial porous membranes made from PTFE and PVDF is provided in Fig. S9 in Supplementary information. It can be seen that the newly prepared PVDF membranes show the highest WVTR and either also the highest LEP (for the pilot scale membrane) or a relationship between WVTR and LEP which is superior (for the lab scale membrane), all compared to the other tested membranes. At the same time, the mechanical stability had been large increased by the integration of the nonwoven support. However, since the supported porous PVDF membrane from this work has been prepared without major optimization of VIPS fabrication conditions, there is still significant room for further improvement.

4. Conclusions

Preparation of porous PVDF membranes with tunable structure and properties via water vapor induced phase separation using the non-hazardous solvent DMSO has been done. In order to tune membrane characteristics to suit an industrial preparation, several process parameters and conditions have been subject of this research, such as kind of a solvent, the molecular weight of the PVDF, the exposure time to the

Table 5
Characteristics for supported porous PVDF membrane fabricated on a pilot scale roll-to-roll system in comparison with porous PVDF membrane prepared under analogous VIPS conditions in lab-scale.

Conditions	Mean flow pore size [µm]	Maximum pore size [µm]	Thickness [µm]	LEP [bar]	WVTR [g/m^{2}h]
Pilot scale 15% PVDF Solef 6010; 150 µm; t_{VIPS} = 104 s	0.13 − 0.18	0.22 − 0.30	114 − 164	2.3 − 4.7	250
Lab scale 15% PVDF Solef 6010; 200 µm; t_{VIPS} = 63 s	0.24	0.59	98	2.7	250

non-solvent (water) vapor, the relative humidity, the polymer concentration and the casting temperature. Overall, it has been shown, that preparation of isotropic porous PVDF membranes with different mean barrier pore sizes in the range from 0.1 to 1 μm is possible within short VIPS time (< 2 min). Based on the detailed knowledge gained in the lab scale studies, PVDF membranes with desired characteristics for some specific gas/liquid membrane contact applications (here mean barrier pore size ~ 0.2 μm) have been prepared on a roll-to-roll system using a nonwoven support. Hence the combination of PVDF, DMSO and VIPS is suggested to be very valuable for industrial membrane production.

Acknowledgements

This work was supported by the EU Horizon 2020 project "XERIC – Innovative Climate – Control System to Extend Range of Electric Vehicles and Improve Comfort" (H2020 - GV - 2014/GV – 2–2014/RIA no. 653605). The discussions with Dr. Nino Gaeta and Dr. Luca Querze from GVS Filter Technology, Zola Predosa (BO), Italy, are gratefully acknowledged. The authors also gratefully acknowledge Smail Boukercha (Anorganische Chemie, Universität Duisburg Essen) for his contribution to the SEM measurements and Yorick Wrausmann for his long-lasting support in laboratory work. The authors also thank Solvay Specialty Polymers Germany GmbH, for supplying the PVDF and GVS Filter Technology for supplying the nonwoven.

Appendix A. Supplementary material

Supplementary data associated with this article can be found in the online version at doi:10.1016/j.memsci.2019.01.033.

References

[1] Z. Cui, E. Drioli, Y.M. Lee, Recent progress in fluoropolymers for membranes, Prog. Polym. Sci. 39 (2014) 164–198.
[2] R. Baker, Membrane Technology and Applications, 2nd ed., Wiley, Menlo Park, California, 2004.
[3] M. Mulder, Basic Principles of Membrane Technology, 2nd ed., Kluwer Academic Publishers, Dordrecht, 1996.
[4] K. Yu Wang, T.-S. Chung, M. Gryta, Hydrophobic PVDF hollow fiber membranes with narrow pore size distribution and ultra-thin skin for the fresh water production through membrane distillation, Chem. Eng. Sci. 63 (2008) 2587–2594.
[5] D. Sun, M.-Q. Liu, J.-H. Guo, J.-Y. Zhang, B.-B. Li, D.-Y. Li, Preparation and characterization of PDMS-PVDF hydrophobic microporous membrane for membrane distillation, Desalination 370 (2015) 63–71.
[6] S. Nejati, C. Boo, C.O. Osuji, M. Elimelech, Engineering flat sheet microporous PVDF films for membrane distillation, J. Membr. Sci. 492 (2015) 355–363.
[7] S. Munirasu, F. Banat, A.A. Durrani, M.A. Haija, Intrinsically superhydrophobic PVDF membrane by phase inversion for membrane distillation, Desalination 417 (2017) 77–86.
[8] C.-Y. Kuo, H.-N. Lin, H.-A. Tsai, D.-M. Wang, J.-Y. Lai, Fabrication of a high hydrophobic PVDF membrane via nonsolvent induced phase separation, Desalination 233 (2008) 40–47.
[9] D. Hou, G. Dai, J. Wang, H. Fan, L. Zhang, Z. Luan, Preparation and characterization of PVDF/nonwoven fabric flat-sheet composite membranes for desalination through direct contact membrane distillation, Sep. Purif. Technol. 101 (2012) 1–10.
[10] A. Gugliuzza, E. Drioli, PVDF and HYFLON AD membranes: ideal interfaces for contactor applications, J. Membr. Sci. 300 (2007) 51–62.
[11] G. Kang, Y. Cao, Application and modification of poly(vinylidene fluoride) (PVDF) membranes – a review, J. Membr. Sci. 463 (2014) 145–165.
[12] M. Khayet, Membranes and theoretical modeling of membrane distillation: a review, Adv. Colloid Interface Sci. 164 (2011) 56–88.
[13] F. Liu, N.A. Hashim, Y. Liu, M.M. Abed, K. Li, Progress in the production and modification of PVDF membranes, J. Membr. Sci. 375 (2011) 1–27.
[14] M. Khayet, C.Y. Feng, K.C. Khulbe, T. Matsuura, Study on the effect of a non-solvent additive on the morphology and performance of ultrafiltration hollow-fiber membranes, Desalination 148 (2002) 321–327.
[15] R. Naim, A.F. Ismail, A. Mansourizadeh, Effect of non-solvent additives on the structure and performance of PVDF hollow fiber membrane contactor for CO_2 stripping, J. Membr. Sci. 423–424 (2012) 503–513.
[16] Q. Li, Z.-L. Xu, M. Liu, Preparation and characterization of PVDF microporous membrane with highly hydrophobic surface, Polym. Adv. Technol. 22 (2011) 520–531.
[17] A. Venault, Y. Chang, J.-R. Wu, D.-M. Wang, Influence of solvent composition and non-solvent activity on the crystalline morphology of PVDF membranes prepared by VIPS process and on their arising mechanical properties, J. Taiwan Inst. Chem. Eng. 45 (2014) 1087–1097.
[18] C.-L. Li, D.-M. Wang, A. Deratani, D. Quémener, D. Bouyer, J.-Y. Lai, Insight into the preparation of poly(vinylidene fluoride) membranes by vapor-induced phase separation, J. Membr. Sci. 361 (2010) 154–166.
[19] M. Li, I. Katsouras, C. Piliego, G. Glasser, I. Lieberwirth, P.W.M. Blom, D.M. de Leeuw, Controlling the microstructure of poly(vinylidene-fluoride) (PVDF) thin films for microelectronics, J. Mater. Chem. C 1 (2013) 7695.
[20] R. Zsigmondy, W. Bachmann, Filter and method of producing same: US Patent, 1922.
[21] P. Menut, Y.S. Su, W. Chinpa, C. Pochat-Bohatier, A. Deratani, D.M. Wang, P. Huguet, C.Y. Kuo, J.Y. Lai, C. Dupuy, A top surface liquid layer during membrane formation using vapor-induced phase separation (VIPS)—Evidence and mechanism of formation, J. Membr. Sci. 310 (2008) 278–288.
[22] M.B. Thürmer, P. Poletto, M. Marcolin, J. Duarte, M. Zeni, Effect of non-solvents used in the coagulation bath on morphology of PVDF membranes, Mater. Res. 15 (2012) 884–890.
[23] T.-H. Young, L.-P. Cheng, D.-J. Lin, L. Fane, W.-Y. Chuang, Mechanisms of PVDF membrane formation by immersion-precipitation in soft (1-octanol) and harsh (water) nonsolvents, Polymer 40 (1999) 5315–5323.
[24] H. Zhang, B. Li, D. Sun, D. Li, J. Li, X. Shao, Effect of the exposure time on the structure and performance of hydrophobic polydimethylsiloxane-poly(vinylidene fluoride) membranes via a non-solvent-induced phase separation process in a clean room, J. Appl. Polym. Sci. 133 (2016) 145.
[25] J.T. Tsai, Y.S. Su, D.M. Wang, J.L. Kuo, J.Y. Lai, A. Deratani, Retainment of pore connectivity in membranes prepared with vapor-induced phase separation, J. Membr. Sci. 362 (2010) 360–373.
[26] H. Chae Park, Y. Po Kim, H. Yong Kim, Y. Soo Kang, Membrane formation by water vapor induced phase inversion, J. Membr. Sci. 156 (1999) 169–178.
[27] H. Fan, Y. Peng, Z. Li, P. Chen, Q. Jiang, S. Wang, Preparation and characterization of hydrophobic PVDF membranes by vapor-induced phase separation and application in vacuum membrane distillation, J. Polym. Res. 20 (2013) 567.
[28] Q. Zhao, R. Xie, F. Luo, Y. Faraj, Z. Liu, X.-J. Ju, W. Wang, L.-Y. Chu, Preparation of high strength poly(vinylidene fluoride) porous membranes with cellular structure via vapor-induced phase separation, J. Membr. Sci. 549 (2018) 151–164.
[29] F.A. AlMarzooqi, M.R. Bilad, H.A. Arafat, Improving liquid entry pressure of polyvinylidene fluoride (PVDF) membranes by exploiting the role of fabrication parameters in vapor-induced phase separation VIPS and non-solvent-induced phase separation (NIPS) processes, Appl. Sci. 7 (2017) 181.
[30] A.L. Ahmad, W.K.W. Ramli, Hydrophobic PVDF membrane via two-stage soft coagulation bath system for Membrane Gas Absorption of CO_2, Sep. Purif. Technol. 103 (2013) 230–240.
[31] A. Bottino, G. Camera-Roda, The formation of microporous polyvinylidene difluoride membranes by phase separation, J. Membr. Sci. (1991) 1–20.
[32] REACH, Candidate List of Substances of Very High Concern for Authorisation, ⟨https://echa.europa.eu/candidate-list-table⟩, (Accessed 1 July 2018).
[33] M.G. Buonomenna, P. Macchi, M. Davoli, E. Drioli, Poly(vinylidene fluoride) membranes by phase inversion: the role the casting and coagulation conditions play in their morphology, crystalline structure and properties, Eur. Polym. J. 43 (2007) 1557–1572.
[34] H.-H. Chang, L.-K. Chang, C.-D. Yang, D.-J. Lin, L.-P. Cheng, Effect of polar rotation on the formation of porous poly(vinylidene fluoride) membranes by immersion precipitation in an alcohol bath, J. Membr. Sci. 513 (2016) 186–196.
[35] Y. Yip, A.J. McHugh, Modeling and simulation of nonsolvent vapor-induced phase separation, J. Membr. Sci. 271 (2006) 163–176.
[36] C. Meringolo, T.F. Mastropietro, T. Poerio, E. Fontananova, G. de Filpo, E. Curcio, G. Di Profio, Tailoring PVDF membranes surface topography and hydrophobicity by a sustainable two-steps phase separation process, ACS Sustain. Chem. Eng. (2018) 10069–10077.
[37] E. McCullough, A comparison of standard methods for measuring water vapour permeability of fabrics, Meas. Sci. Technol. (2003) 1402–1408.
[38] C.M. Hansen, Hansen Solubility Parameters: A User's Handbook, 2nd ed., Taylor & Francis.
[39] D.J. Lin, K. Beltsios, T.H. Young, Y.S. Jeng, L.P. Cheng, Strong effect of precursor preparation on the morphology of semicrystalline phase inversion poly(vinylidene fluoride) membranes, J. Membr. Sci. 274 (2006) 64–72.
[40] Y.-M. Wei, Mathematical calculation of binodal curves of a polymer/solvent/non-solvent system in the phase inversion process, Desalination 192 (2006) 91–104.
[41] H. Strathmann, K. Kock, The formation mechanism of phase inversion membranes, Desalination 21 (1977) 241–255.
[42] L.-J. Zhu, H.-M. Song, G. Wang, Z.-X. Zeng, C.-T. Zhao, Q.-J. Xue, X.-P. Guo, Microstructures and performances of pegylated polysulfone membranes from an in situ synthesized solution via vapor induced phase separation approach, J. Colloid Interface Sci. 515 (2018) 152–159.
[43] L. Zhu, H. Song, G. Wang, Z. Zeng, Q. Xue, Symmetrical polysulfone/poly(acrylic acid) porous membranes with uniform wormlike morphology and pH responsibility: preparation, characterization and application in water purification, J. Membr. Sci. 549 (2018) 515–522.
[44] D.G.A.L. Aarts, R.P.A. Dullens, H.N.W. Lekkerkerker, Interfacial dynamics in demixing systems with ultralow interfacial tension, New J. Phys. 7 (2005) 40.